The Canadian Mineralogist
Vol. 31, pp. 957-971 (1993)

CLAY MINERALOGY OF ACTIVE HYDROTHERMAL CHIMNEYS AND AN ASSOCIATED MOUND, MIDDLE VALLEY, NORTHERN JUAN DE FUCA RIDGE*

JEANNE B. PERCIVAL AND DOREEN E. AMES

Geological Survey of Canada, 601 Booth Street, Ottawa, Ontario K1A 0E8

ABSTRACT

Active hydrothermal sites were sampled during 1990 in a series of ALVIN dives in the Middle Valley area of the northern Juan de Fuca Ridge. This study focused on the hydrothermal clay minerals precipitated within active anhydrite-rich and sulfide-bearing chimneys and an active hydrothermal mound at the Area of Active Venting (AAV) and Bent Hill sites. Based on XRD, SEM, ATEM and electron-microprobe results, the dominant clay mineral in the chimneys is saponite. In the AAV, Fe-rich saponite, Fe-rich smectite and chlorite also were observed in trace to minor amounts. Smectite occurs only as a mixed-layer component, with either illite or chlorite at Bent Hill. The Central Site hydrothermal mound in the AAV contains lizardite, saponite and possibly a mixed-layer mineral of these two phases. The clay minerals were directly precipitated in the active vents and hydrothermal mound by interaction of cold Mg-rich seawater and moderately hot (< 276°C) hydrothermal fluids with a low $f(O_2)$ and Si activity.

Keywords: seafloor, sediment-covered rift, active chimneys, hydrothermal precipitates, clay mineralogy, smectite, saponite, serpentine, lizardite, Middle Valley, Juan de Fuca Ridge.

SOMMAIRE

Les sites actifs d'activité hydrothermale de la région de Middle Valley, dans le secteur nord de la dorsale Juan de Fuca, ont été échantillonnés en 1990, par une série de plongées avec le submersible ALVIN. Nous avons porté notre attention sur les argiles précipitées à l'intérieur de cheminées actives riches en anhydrite et porteuses de sulfures, et aussi dans une culmination hydrothermale active dans les sites dits Area of Active Venting (AAV) et Bent Hill. A la lumière de nos résultats, obtenus par diffraction X, microscopie électronique à balayage et par transmission (mode analytique), et par microsonde électronique, le minéral prédominant semble être la saponite. Dans la zone AAV, saponite ferrifère, un deuxième membre ferrifère du groupe de la smectite, et chlorite ont aussi été trouvés, en quantités moindres. A Bent Hill, les minéraux du groupe de la smectite sont présents seulement sous forme de composant d'un minéral interstratifié, avec illite ou chlorite. Dans la zone AAV, l'amoncellement dit Central Site contient lizardite, saponite, et une espèce interstratifiée qui contiendrait ces deux phases. Les argiles ont été précipitées directement dans les évents actifs et l'amoncellement hydrothermal suite à l'interaction de l'eau de mer, froide et riche en Mg, avec une phase hydrothermale à température moyenne (<276°C) et à activité de Si et fugacité d'oxygène faibles.

(Traduit par la Rédaction)

Mots-clés: fond océanique, rift rempli de sédiments, cheminées actives, précipités hydrothermaux, minéralogie des argiles, minéral du groupe de la smectite, saponite, serpentine, lizardite, Middle Valley, dorsale de Juan de Fuca.

INTRODUCTION

During 1990, a series of five ALVIN dives explored the Middle Valley area of the northern Juan de Fuca Ridge, to map and collect samples of the active hydrothermal sites and inactive massive sulfide deposits, prior to ocean drilling (ODP Leg 139). Middle Valley is a 15-km-wide failed rift, at a water depth of 2400 m, filled with Pleistocene turbiditic sediments derived from the North American continental margin. The sediment-filled rift is located at the intersection of the Endeavour segment of the Juan de Fuca Ridge and the Sovanco Transform Fault, about 200 km west of the continental margin off the British Columbia coast (Fig. 1).

Two areas of hydrothermal activity are known near the eastern margin of Middle Valley: the Area of Active Venting (AAV), which contains at least 20

---

* Geological Survey of Canada contribution number 43092.

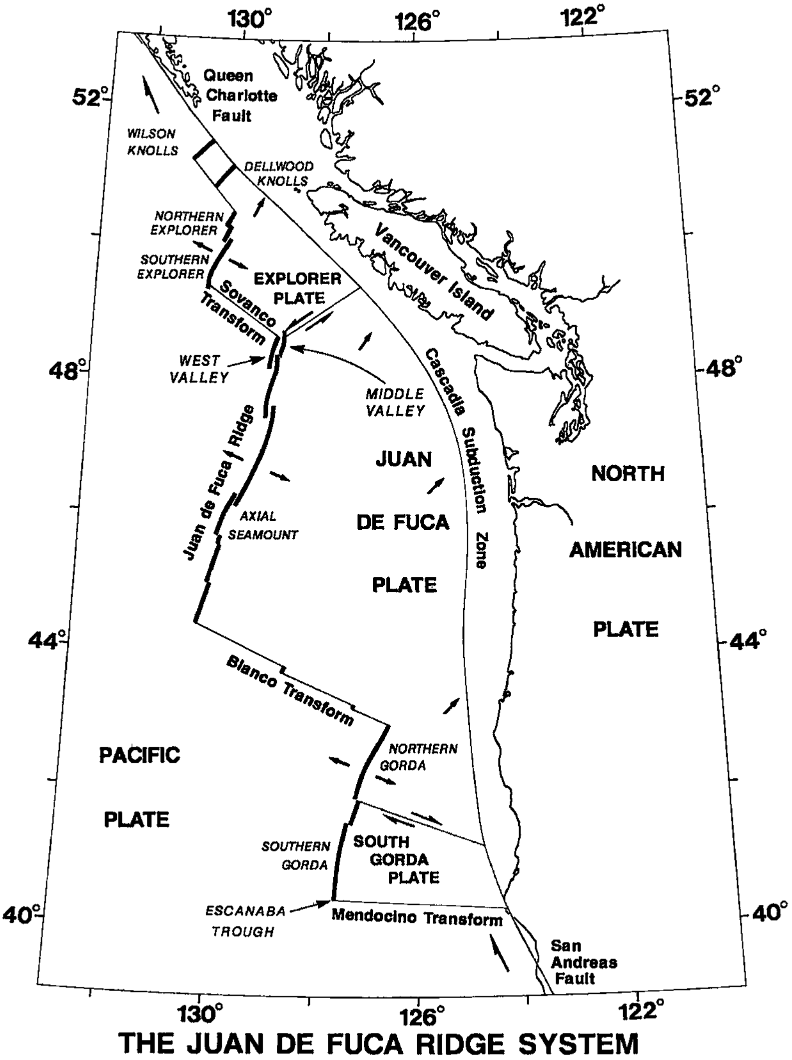

FIG. 1. Location of Middle Valley, northern Juan de Fuca Ridge.

active vent sites and a heat flow anomaly, and Bent Hill, which contains two inactive massive sulfide deposits and only one observed active vent (Davis *et al.* 1987, Goodfellow & Blaise 1988, Ames *et al.* 1993) (Fig. 2). The AAV is an 800 m by 350 m, north-trending, rift-parallel zone situated over a local basement high (Ames *et al.* 1993). Moderate-temperature hydrothermal fluids (184° $< T <$ 276°C) emanate from vents at the top of a series of hydrothermal mounds averaging 25 m across and 7 m high. The mound slopes are composed of hydrothermal precipitates, altered sediment and toppled chimneys (vents), and are partially covered at the base by bacterial mats with clams and tube worms. Bent Hill, located about 3 km southeast of the AAV, consists of a subcircular, uplifted block of sediment about 500 m in diameter, rising 60 m above the relatively flat floor of Middle Valley. Sulfide deposits occur less than 50 m to the south (Franklin *et al.* 1991). An active chimney, 360 m south of Bent Hill, is spatially associated with a small mound of massive sulfide (Ames *et al.* 1993).

Sediment alteration was documented for the near-surface samples from piston cores penetrating <12 m of sediment (Davis *et al.* 1987, Goodfellow & Blaise

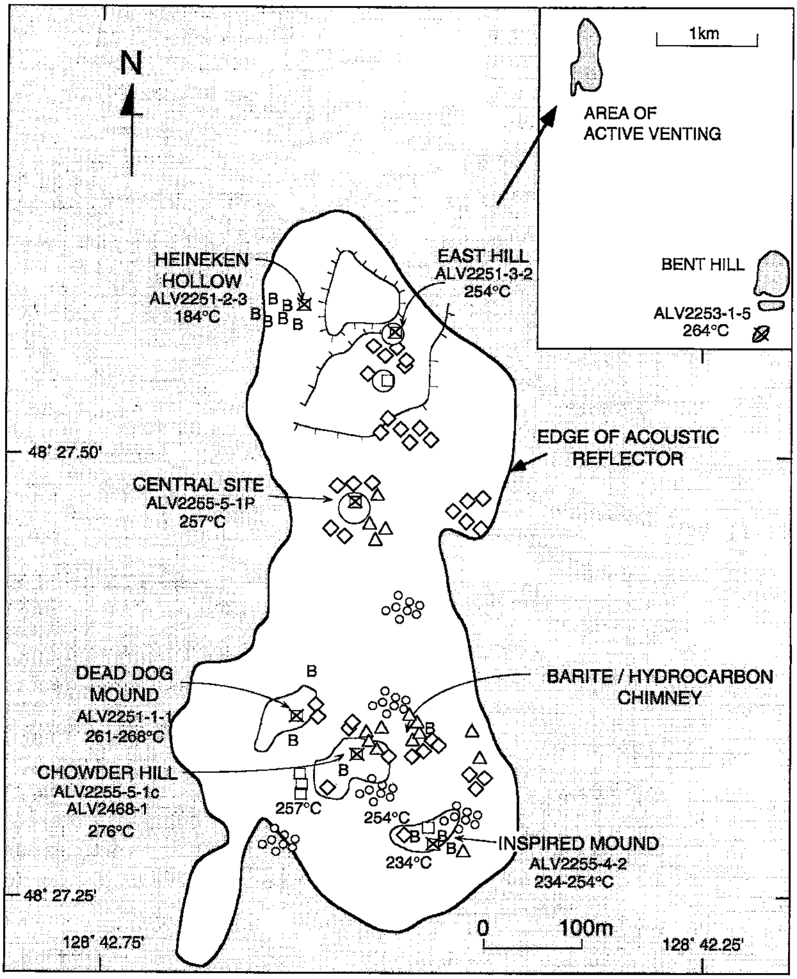

FIG. 2. Location of sample sites within the Area of Active Venting (AAV) and Bent Hill. Sample numbers (*e.g.*, 2255–5–1) indicates dive (2255), station (5) and specimen (1) numbers, respectively. "P" designation at the end of the sample number indicates push core.

1988) and from push cores of surface sediment (<0.5 m) (Turner *et al.* 1993). Detailed studies of the mineralogy and chemistry of mound and sulfide deposits, and active and inactive chimneys in the two hydrothermal areas at Middle Valley, are reported in Ames & Franklin (1992) and Ames *et al.* (1993). The mineralogical and chemical composition of the sulfate-rich active hydrothermal chimneys reflects significant fluid–sediment interaction, whereas the massive sulfide deposits were probably derived from the reaction of modified seawater with high-temperature basaltic basement (Ames *et al.* 1993).

Clay minerals in active hydrothermal systems have received less study than sulfides owing to their complexity and fine grain-size. The present study, complementary to that of Ames *et al.* (1993), addresses the nature of hydrothermal clay minerals precipitated within the active chimneys and associated mounds, the origin of the clays and their relationship to clays from other active hydrothermal areas. Material recovered from active chimneys provides an excellent opportunity to study processes of precipitation from hydrothermal fluids.

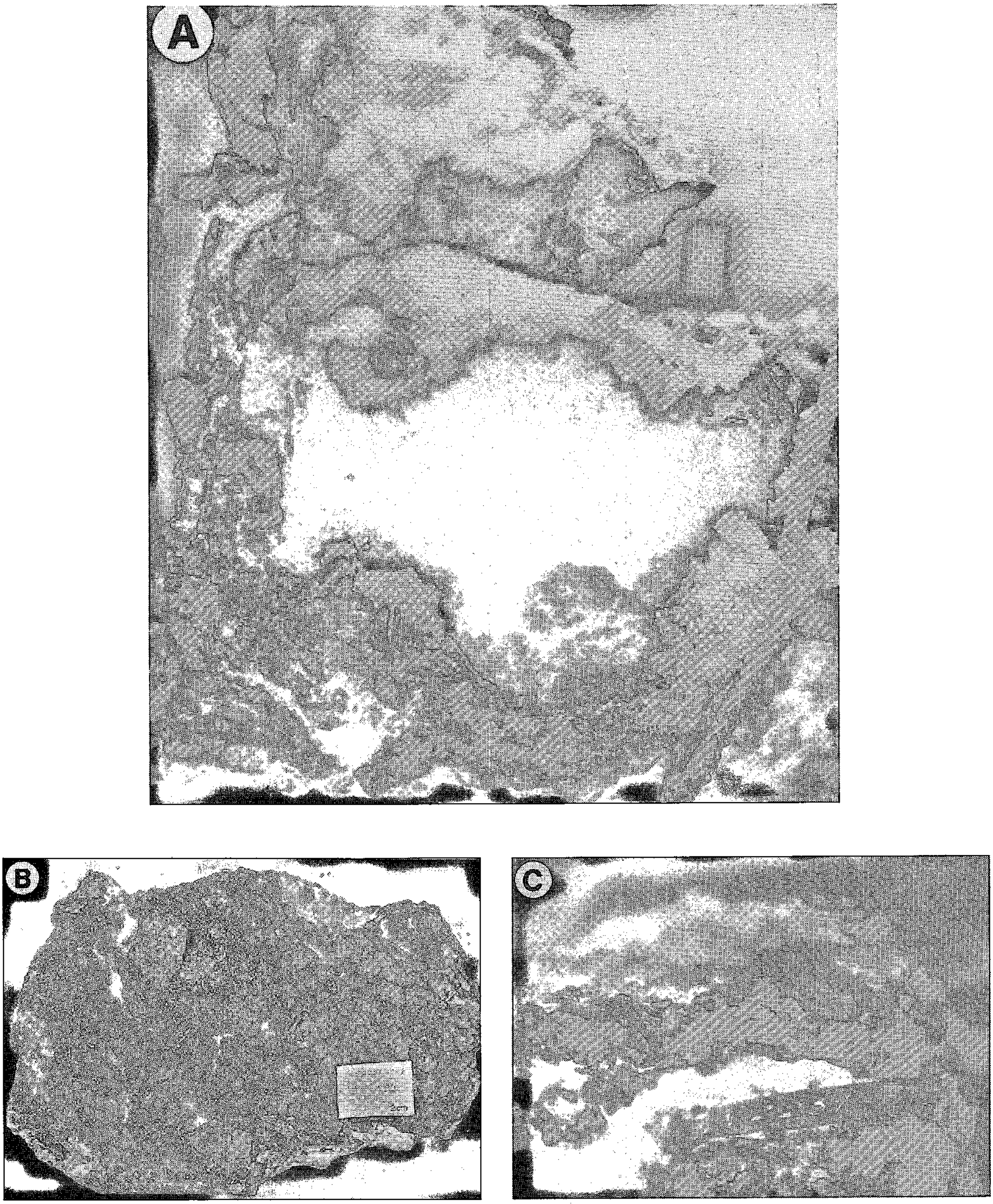

FIG. 3. The active chimneys at Middle Valley are all similar to that at Dead Dog Mound (A, B and C), with chimney structure composed dominantly of white, pale grey and purplish anhydrite, with a central, black-coated surface of Mg-rich smectite and very fine-grained sulfides. The 5% sulfides in the chimney lining are dominated by pyrrhotite, chalcopyrite and isocubanite, with lesser sphalerite, barite and galena. A. Cross-sectional view down the chimney orifice. B. Planar view of lobate smectite–sulfide lining of chimney orifice; hydrothermal fluid pathway. C. Note the thin, < 2 mm, black clay–sulfide lining. This material is the focus of this study.

DESCRIPTIONS OF SAMPLES AND SITES

Chimney samples and a push-core sample were selected from seven sites within the two hydrothermal areas (Fig. 2). The active chimneys were sampled using the mechanical arm of ALVIN during dives 2251 to 2255 by the chief scientist, J.M. Franklin (Geological Survey of Canada), and other members of the dive cruise, and during dive 2468 by M.D. Hannington (Geological Survey of Canada) in 1991.

Preliminary mapping in the AAV shows groupings of active vents in the north and south (Fig. 2). In the northwestern part of the AAV, a depression 3 to 5 m in diameter referred to as Heineken Hollow contains a small, central, active chimney. Diffuse, clear, hydrothermal fluids (T = 184°C) flow through cracks in barite-rich crusts within the depression. Sample ALV2251–2–3 from Heineken Hollow is typical of material making up the active chimneys, and is composed predominantly of anhydrite. On the eastern side of the AAV a large, smooth-sided mound, East Hill, has a vigorously venting anhydrite-rich chimney (sample ALV2251–3–2). Clear fluids emanate from the top of the chimney at 250°C.

Near the center of the AAV (Central Site), an active vent, at 257°C, occurs on top of a large mound in the middle of inactive barite-rich chimneys. Slightly greyish fluids were discharging from a large spire (2 m high × 75 cm across) and also were leaking from the base. Push core ALV2255–5–1P was taken from the Central Site active hydrothermal mound at the base of the chimney. It consists of a 4-cm-thick cap of anhydrite with minor gypsum and sulfide, underlain by 5 cm of massive sulfide with chalcopyrite, pyrite, sphalerite and galena, with minor anhydrite and serpentine. A 5-cm-wide zone of white gel composed of clay, barite, chalcopyrite, sphalerite and galena forms the basal layer (Turner *et al.* 1993). This basal white gel was sampled for detailed characterization of the clays within active hydrothermal mounds.

Dead Dog Mound, in the southwestern corner of the AAV, is topped by large, 5- to 6-m-high anhydrite-rich chimneys (samples ALV2251–1–1 and ALV2251–1–1a). Clear fluids flow at 261°C from the top of the chimneys. The core of the chimneys contain asymmetrical bulbous masses of clay with minor pyrrhotite, chalcopyrite and sphalerite and galena (Figs. 3A, B). The asymmetry and slight imbrication of the bulbous clay deposits record the direction of fluid flow up the chimney.

The large chimney on Chowder Hill was found to be venting greyish hydrothermal fluids emanating at 276°C, the highest temperature measured in Middle Valley. Mineralogically, the Chowder Hill chimney (samples ALV2252–5–1c and ALV2468–1) is similar to the others, but contains a higher proportion of sulfide minerals (5 – 10 vol. %).

Inspired Mound consists of a group of mounds, one of which is large, with three chimneys venting clear hydrothermal fluids at 234 to 254°C. Sample ALV2255–4–2 is typical of the active chimneys in Middle Valley, but has a higher Pb content, reflected in the presence of galena (Ames *et al.* 1993). The sample is heterogeneous, without apparent systematic zoning.

In the Bent Hill area, the one active chimney is situated on a domed surface 2 to 5 m in diameter that vents 264°C fluid from the base of the chimney. Adjacent to the active chimney is a higher outcrop of massive sulfide. Small fragments of the active chimney (sample ALV2253–1–5) were recovered.

ANALYTICAL METHODS

Suitable material for analysis of clay minerals was obtained from the scrapings of the inner wall of the active chimneys and the white, gel-like material from the Central Site hydrothermal mound. The clay-size fraction (<2 μm) was separated from the bulk material by centrifugation. Suspensions of the clay fraction and bulk samples were pipetted onto glass slides and air-dried overnight to produce oriented mounts. X-ray patterns of the air-dried samples were recorded on a Philips PW1710 automated powder diffractometer equipped with a graphite monochromator, Cu$K\alpha$ radiation and a Ni filter at 50 kV and 30 mA. The samples were also X-rayed following saturation with ethylene glycol and heat treatment (550°C).

Polished thin sections and grain mounts of some samples were prepared for petrographic and scanning electron microscopy, and electron-microprobe analyses. We used a Cambridge S–200 scanning electron microscope (SEM) equipped with a Link Analytical AN10000 integrated energy-dispersion X-ray analyzer (EDX) and back-scattered electron detector.

The composition of the clays was determined from polished thin sections using CAMEBAX and CAMECA SX–50 electron microprobes with wavelength-dispersion spectrometers, operating at an accelerating voltage of 15 kV and regulated beam currents of 10 nA, with a 10-μm beam. The data were processed with a øρZ (Phi–Rho–Z) type of correction program using oxide standards. Structural formulae based on 22 oxygen equivalents were calculated using an in-house computer program (G. Pringle, pers. comm., 1992), with the assumption that all iron is present as ferrous iron. This assumption is supported by the presence of sulfide minerals with the clays (Ames *et al.* 1993). Excess charges at the tetrahedral and octahedral positions were calculated according to the method of Moore & Reynolds (1989).

Samples were prepared for analytical transmission electron microscopy (ATEM) by pipetting one drop of a very dilute suspension of <2 μm sample onto carbon-coated Cu-grids. The samples were analyzed using a Hitachi H–800 Electron Microscope at the

University of Toronto with an H–8010 scanning system, with 200 kV accelerating voltage and 2 μA current. This instrument was equipped with a Kevex EDX system and Tracor Northern computer for qualitative X-ray analysis.

RESULTS

Distribution of clay minerals

Petrographic data provide an overview of the mineralogy of the samples (Table 1); more detailed petrography of the active chimneys is provided in Ames *et al.* (1993). The chimneys have an outer zone composed of anhydrite, with minor to trace gypsum, bassanite [identified through whole-rock X-ray diffraction (XRD)] and sulfides, and an inner core lining, 2 mm wide, composed dominantly of clay (up to 70% by volume; Fig. 3C). Finely disseminated sulfide minerals, pyrrhotite, pyrite, marcasite, isocubanite, chalcopyrite, sphalerite and galena, also occur in minor to trace amounts in the inner lining. Clay material accounts for only 2 – 5% by volume of the entire chimney. The fluid channelways of the chimneys are surrounded by an outer zone of anhydrite that is usually more than 10 cm thick.

The mineral assemblages inferred by XRD are given in Table 2. The clay material lining the core of the active chimneys and the mound sample is dominantly a smectite-group mineral. It is intimately associated with sulfides in the inner zone and replaces anhydrite in the outer zone of the chimney lining (Fig. 4). Figure 4A shows a cross-section of the smectite–sulfide lining of the active chimney from Dead Dog Mound. In this photomicrograph, the bulbous aggregates of clay minerals, oriented convexly toward the fluid pathway, occur in alternating fine bands with chalcopyrite, sphalerite and pyrrhotite (bright grains). Figure 4B reveals the bulbous nature and typical crenulated morphology of the smectite globules. In the anhydrite-rich outer zone of the chimney lining, smectite forms casts of the lath-shaped anhydrite along minor fluid pathways (Figs. 4C, D).

TABLE 1. MINERALOGY OF CHIMNEY AND PUSH CORE SAMPLES BASED ON PETROGRAPHIC ANALYSES

SAMPLE SITE	VENT TEMP.(°C)	MINERALOGY	ABUNDANCE
AAV			
CENTRAL SITE	< 100	Clay	A
ALV2255-5-1P1		Brt, Ccp,	M-T
ALV2255-5-1P2		Gn, Sp, Mrc	T
HEINEKEN HOLLOW	184	Anh	A
ALV2251-2-3		Clay	M
		Brt, Ccp, Sp, Gn	T
EAST HILL	254	Anh	A
ALV2251-3-2		Gp, Bas	M
		Ccp, Sp, Brt, Gn	T
INSPIRED MOUND	234-254	Anh	A
ALV2255-4-2		Clay	M-T
		Gn, Ccp, Sp	T
DEAD DOG MOUND	261-268	Anh	A
ALV2251-1-1		Gp	M
ALV2251-1-1a		Clay, Ccp, Po	M-T
		Sp, Gn, Apy	T
CHOWDER HILL	276	Anh	A-M
ALV2255-5-1c		Clay	M
ALV2468-1		Ccp, Po, Sp, Py, Gn	T
BENT HILL			
ALV2253-1-5	264	Anh	A
		Po, Ccp, Clay	T

Anh: Anhydrite, Apy: Arsenopyrite, Bas: Bassanite, Brt: Barite, Ccp: Chalcopyrite, Gn: Galena, Gp: Gypsum, Mrc: Marcasite, Po: Pyrrhotite, Py: Pyrite, Sp: Sphalerite.
A: Abundant, M: Minor, T: Trace.
P in sample number indicates push core.

TABLE 2. MINERALOGY OF CHIMNEY AND PUSH CORE SAMPLES BASED ON XRD AND SEM ANALYSES

SAMPLE SITE	BULK MINERALOGY	CLAY MINERALOGY	ABUNDANCE
AAV			
CENTRAL SITE		Srp	A
ALV2255-5-1P1		Sm	A-M
ALV2255-5-1P2		Srp/Mg-Sm ML	M-T
HEINEKEN HOLLOW	Sm	Ccp, Sm	A
ALV2251-2-3	Ccp		A-M
	Tlc	Amo	T
EAST HILL	Sm	Sm	A
ALV2251-3-2	Ccp, Anh	Ccp	M
	Py	Amo	T
INSPIRED MOUND	Ccp	Anh, Mg-Sm	A
ALV2255-4-2	Anh		A-M
		Ccp	M
	Py, Sm, Gp		T
DEAD DOG MOUND	Sm	Sm	A
ALV2251-1-1	Ccp	Ccp	A-M
ALV2251-1-1a	Anh, Gp		M
	Tlc		T
CHOWDER HILL	Anh	Anh	A
ALV2255-5-2		Chl	M
ALV2468-1	Ccp		M-T
	Gp, Chl, Grg	Sm, Amo, Grg	T
BENT HILL			
ALV2253-1-5	Anh, Gp		A-M

Amo: X-ray Amorphous material (undesignated), Anh: Anhydrite, Ccp: Chalcopyrite, Chl: Chlorite, Grg: Greigite, Gp: Gypsum, ML: Mixed-Layer Clay Mineral, Py: Pyrite, Srp: Serpentine, Sm: Smectite-group mineral, Tlc: Talc.
A: Abundant, M: Minor, T: Trace.
P in sample number indicates push core.

A smectite-group mineral also occurs with serpentine in the low-temperature push-core sample from the Central Site mound and with minor to trace amounts of talc at Heineken Hollow and Dead Dog Mound (Table 2). At Chowder Hill, chlorite appears in the assemblage and is more abundant than the smectite. No clay minerals were detected in bulk samples from Bent Hill.

Figure 5A shows the diffractometer trace of a typical smectite observed in the active chimneys in the AAV. In this sample from Dead Dog Mound, only smectite and chalcopyrite are observed. After heat treatment, the smectite basal spacing collapsed from 17.0, 8.68, 5.64 and 3.37 Å, to 9.79, 4.81 and 3.19 Å. The resultant basal spacings are similar to those of a hydrated talc structure (Drits *et al.* 1989), and suggest

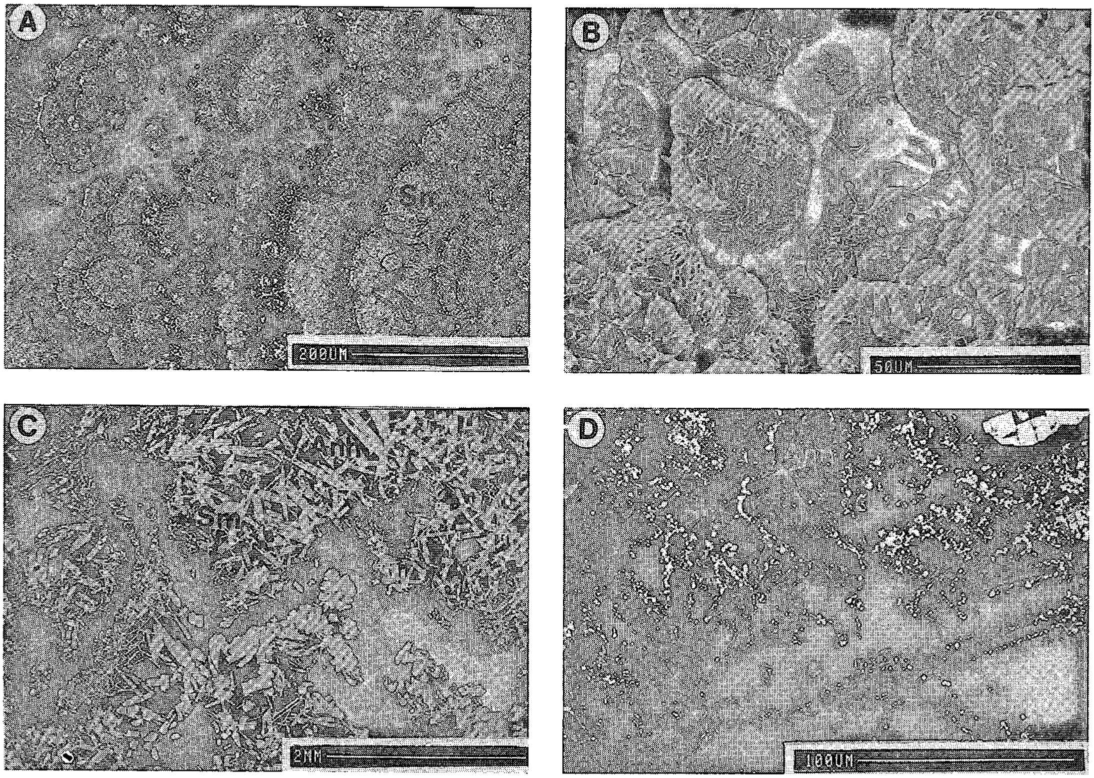

FIG. 4. A. SEM micrograph showing typical cross-sectional view across the smectite–sulfide lining of the chimney. The clay minerals (Sm) are convex toward the fluid pathway; bright grains are sulfides [back-scattered electron image (BSI); bar scale given at bottom of photo]. B. SEM micrograph of mounted fragment from the core of Dead Dog Mound. Note the 40-μm semispherical bulbous smectite. The clay aggregates are convex toward the fluid pathway [secondary electron image (SEI)]. C. Smectite replacement of anhydrite (Anh) is evident in minor pathways of fluid through the anhydrite-rich outer zone. Note the smectite casts of lath-shaped anhydrite (BSI). D. At the contact between the clay-rich portion and the anhydrite outer zone, smectite forms casts of anhydrite. Note the lath-shaped voids (BSI).

that the smectite is Mg-rich. The 060 X-ray peak is observed at 1.53 Å (determined by XRD of a random mount) in one of the Central Site samples. This peak, however, coincides with the 060 X-ray peak of serpentine, also present in this sample.

The diffractometer trace for the Central Site mound sample (ALV2255–5–1P2) is shown in Figure 5B. It consists dominantly of serpentine and smectite, with minor to trace amounts of a serpentine–smectite mixed-layer clay mineral, chalcopyrite and pyrite. Smectite was identified by its expansion from about 14 Å to 17 Å after glycol treatment and its collapse to 10 Å following heat treatment. There is no change in the peak positions for serpentine, but in the diffractogram of the glycolated sample, a shoulder appears on the low-angle side of the 7.4 Å peak at about 7.8 Å, and another appears on the high-angle side of the 3.66 Å peak at 3.57 Å. The behavior of the smectite and serpentine minerals in response to glycolation suggests the presence of a serpentine–smectite mixed-layer mineral in the Central Site hydrothermal mound.

Results of the ATEM analyses (Table 3) confirm the presence of smectite in all samples from the AAV (Fig. 6A). Chlorite, identified by its morphology and EDX spectra, also was observed in chimney samples from East Hill and Bent Hill (Fig. 6B). Trace amounts of mixed-layer clay minerals such as illite–smectite, chlorite–smectite or chlorite–illite are associated with chlorite, as suggested by the presence of trace to minor amounts of K and Ca observed in the EDX spectra.

X-ray-amorphous material, probably silica, was identified in a few samples by a broad hump in the central region of the XRD traces. The ATEM results also indicate the presence of sodic plagioclase in the East Hill chimney lining and of Fe oxide at Chowder Hill.

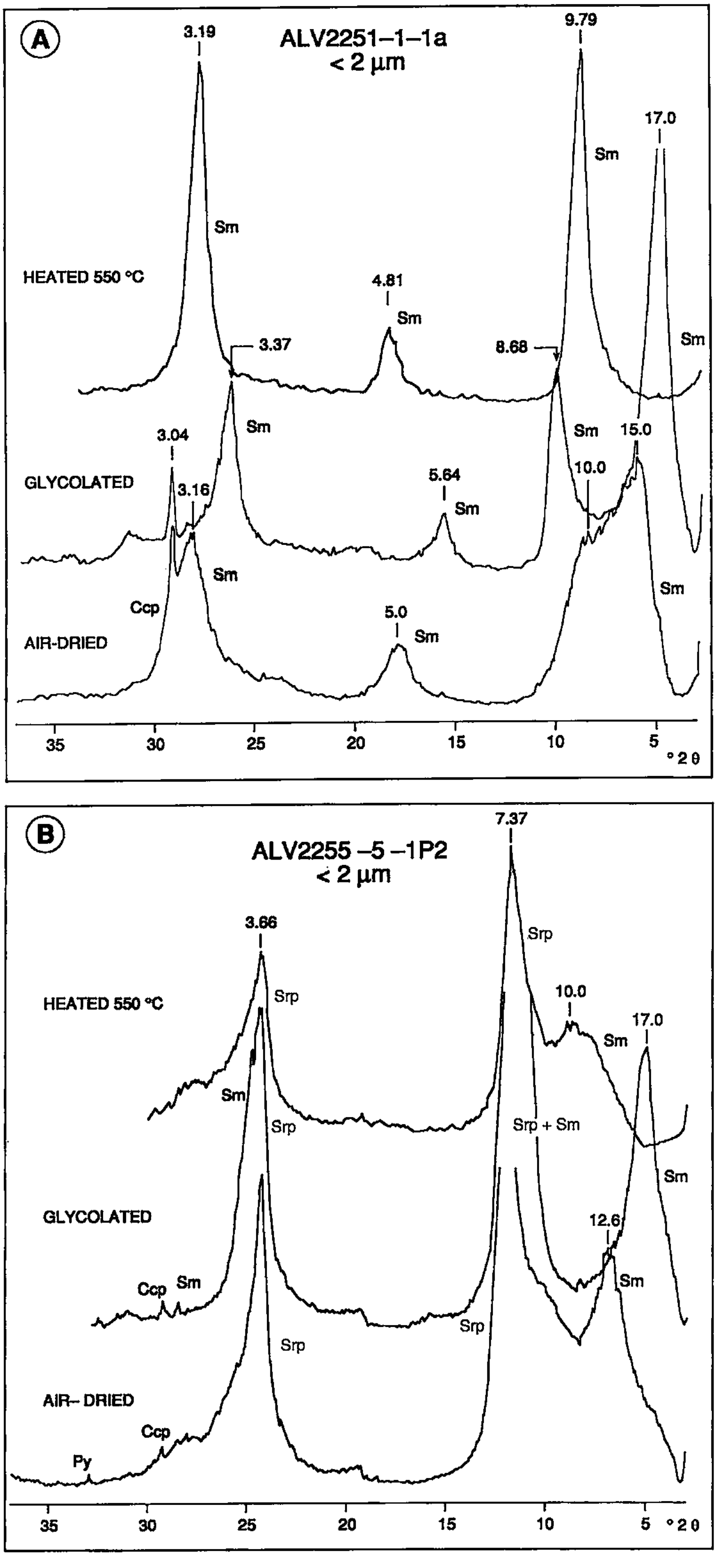

FIG. 5. A. Air-dried, glycolated and heat-treated X-ray-diffraction patterns of clay-size (<2 µm) sample ALV2251-1-1a from Dead Dog Mound. These patterns are typical of the Mg-rich smectite (Sm; saponite) observed in all samples. B. Air-dried, glycolated and heat-treated X-ray-diffraction patterns of clay-size (<2 µm) sample ALV2255-5-1P2 from Central Site. This sample is composed of serpentine (Srp; lizardite), smectite (Sm; saponite), chalcopyrite (Ccp) and pyrite (Py). There is evidence (not shown) for a Srp–Sm mixed-layer clay mineral.

TABLE 3. MINERALOGY OF CHIMNEY AND PUSH CORE SAMPLES BASED ON ATEM ANALYSES

SAMPLE SITE	MINERALOGY
AAV	
CENTRAL SITE ALV2255-5-1P1 ALV2255-5-1P2	Srp, Sm (Sap), Srp/Sm ML
HEINEKEN HOLLOW ALV2251-2-3	Sm (Sap), Co-bearing Sm
EAST HILL ALV2251-3-2	Sm (Sap), Chl, Na-Pl, Chl/Ill ML?
INSPIRED MOUND ALV2255-4-2	Sm (Sap and Fe-Sap), poorly crystalline
DEAD DOG MOUND ALV2251-1-1 ALV2251-1-1a	Sm (Sap and Fe-Sap) poorly crystalline
CHOWDER HILL ALV2255-5-1c ALV2468-1	Chl, Fe-Sm, FeO
BENT HILL	
ALV2253-1-5	Chl, Chl/Ill or Sm ML, Ill/Sm ML, Gp or Anh

Anh: Anhydrite, Chl: Chlorite, FeO: Feoxide, Gp: Gypsum, Ill: Illite, ML: Mixed-Layer Clay Mineral, Pl: Plagioclase, Sap: Saponite, Srp: Serpentine, Sm: Smectite-group mineral.
A: Abundant, M: Minor, T: Trace.
P in sample number indicates push core.

TABLE 4. RESULTS OF ELECTRON-MICROPROBE ANALYSES OF CHIMNEY AND PUSH CORE SAMPLES

	1 (n = 10)	2 (n = 8)	3 (n = 21)	4 (n = 3)	5 (n = 16)	6 (n = 9)
SiO_2 (wt.%)	47.12	48.39	58.09	44.26	48.85	44.79
Al_2O_3	3.26	3.11	1.07	3.76	1.66	4.59
Fe_2O_3	4.24	3.35	0.12	2.27	0.00	1.02
FeO	1.51	0.73	1.81	2.89	3.16	0.00
MnO	0.18	0.09	0.10	0.17	0.14	0.03
MgO	22.95	24.22	28.52	20.90	22.97	28.91
CaO	0.25	0.49	0.13	0.33	0.10	0.46
Na_2O	0.36	0.15	0.23	0.32	0.42	0.69
K_2O	0.07	0.08	0.08	0.08	0.10	0.16
TOTAL	79.94	80.61	90.15	74.98	77.40	80.65
$MgO/(MgO+SiO_2)$	0.33	0.33	0.33	0.32	0.32	0.39
STRUCTURAL FORMULA BASED ON 22 OXYGEN EQUIVALENTS						
Si	7.432	7.481	7.855	7.416	7.776	
Al	0.568	0.519	0.145	0.584	0.224	
	8.000	8.000	8.000	8.000	8.000	
Al	0.038	0.048	0.026	0.159	0.087	
Fe^{2+}	0.701	0.484	0.217	0.691	0.421	
Mn	0.024	0.012	0.011	0.024	0.019	
Mg	5.396	5.582	5.749	5.220	5.450	
	6.159	6.126	6.003	6.094	5.977	
Ca	0.042	0.081	0.019	0.059	0.017	
Na	0.110	0.045	0.060	0.104	0.130	
K	0.014	0.016	0.014	0.017	0.020	
	0.166	0.142	0.093	0.180	0.167	
Tet. Excess Charge	-0.568	-0.519	-0.145	-0.584	-0.224	
Oct. Excess Charge	+0.356	+0.300	+0.032	+0.347	+0.041	
Total Excess Charge	-0.212	-0.219	-0.113	-0.237	-0.183	
Interlayer Charge	+0.208	+0.223	+0.112	+0.239	+0.184	

1. Heineken Hollow, sample ALV2251-2-3. 2. East Hill, sample ALV2251-3-2.
3. Inspired Mound, sample ALV2255-4-2. 4. Dead Dog Mound, sample ALV2251-1-1.
5. Chowder Hill, sample ALV2255-5-1c. 6. Central Site, sample ALV2255-5-1P1.
n = Number of analyses.

Compositions of the clay minerals

Electron-microprobe results and calculated anhydrous structural formulae of smectite grains from each of the sites in the AAV are given in Table 4. A structural formula was not calculated for analysis 6 as it is a fine-grained mixture of serpentine and smectite. The SiO_2 content ranges from about 44 to 58 wt%, and

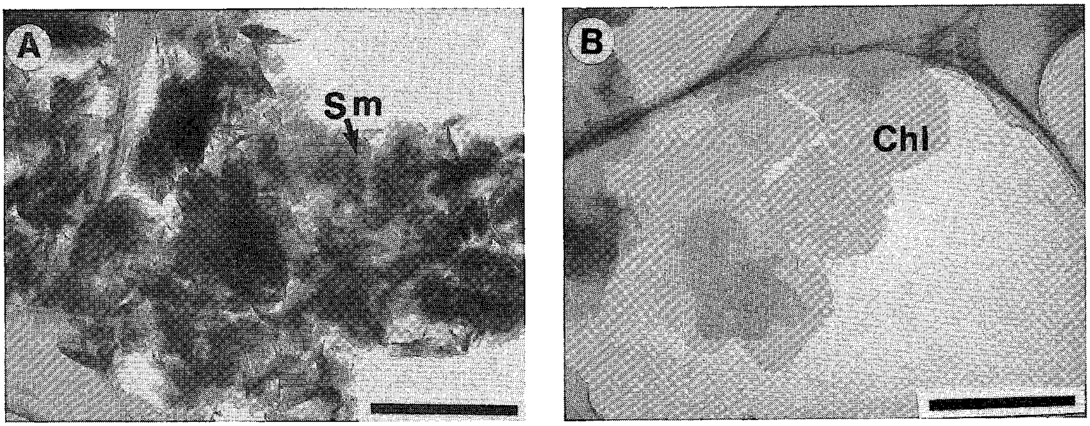

FIG. 6. ATEM micrographs of sample ALV2251–3–2 from East Hill showing typical examples of the morphology of: A) Mg-rich smectite (Sm) and B) chlorite (Chl; Mg–Fe variety) (scale bar: 0.5 μm).

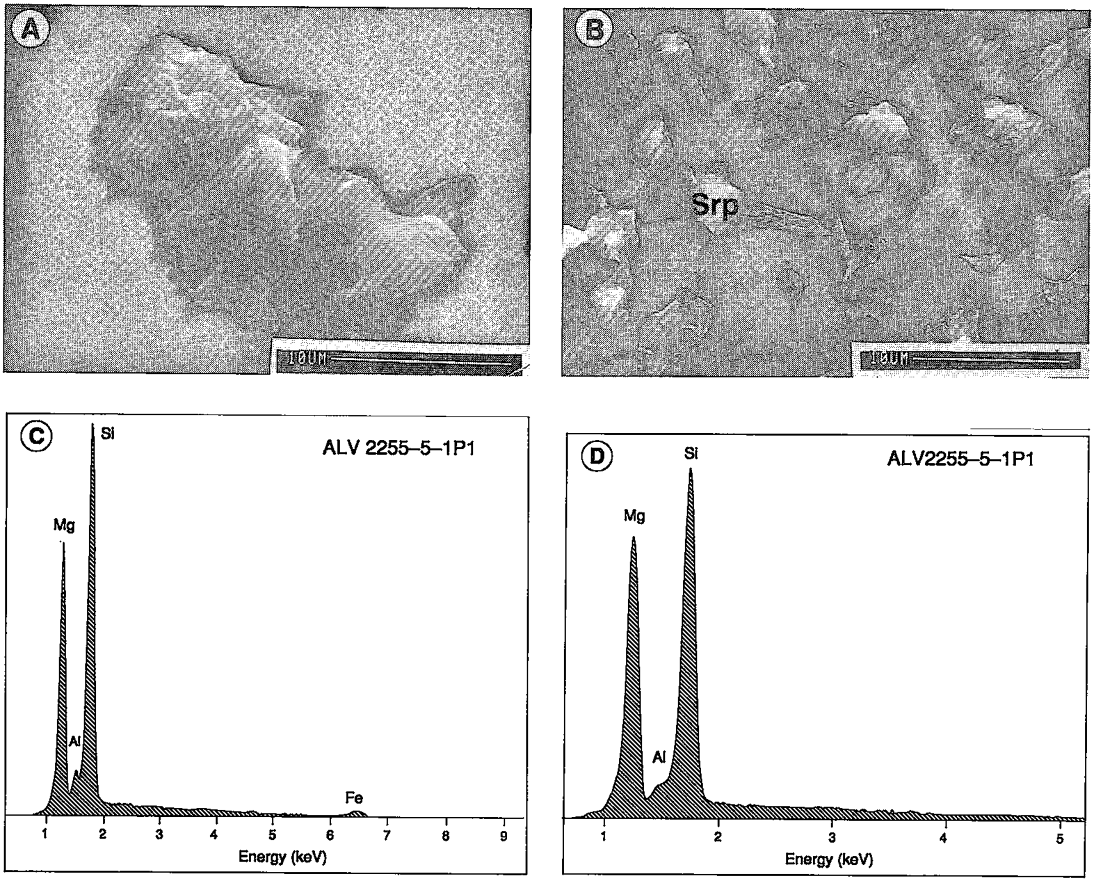

FIG. 7. A. SEM micrograph showing crenulated morphology typical of smectite (grain mount, SEI). Smectite identified by X-ray-diffraction analyses. B. SEM micrograph of smectite (Sm) and serpentine (Srp) (SEI). C. EDX spectrum of smectite (see label) from 7B. D. EDX spectrum for serpentine(?) (see label) from 7B.

MgO, from about 21 to 29 wt%. The MgO/(MgO+SiO_2) ratios, however, are consistent at 0.32–0.33 for all five samples of smectite. The sample from Central Site (analysis 6) is enriched in Mg relative to the other samples. The Al_2O_3 content ranges from about 1 to 4.5 wt%; Al is assumed to occupy the layer of tetrahedra. The substitution of ^{IV}Al for Si and the 060 X-ray peak at 1.53 Å suggest that the dominant smectite observed in all samples is the trioctahedral, Mg-rich variety, saponite. The smectite samples are typically Mg-rich (also defined by XRD, described above), with minor Al and Fe. The idealized formula of saponite, $(1/2\ Ca,Na)_{0.66}(Mg_6)(Si_{7.34}Al_{0.66})O_{20}(OH)_4{\cdot}nH_2O$ (Deer *et al.* 1966), corresponds with analyses 1, 2 and 4 (Heineken Hollow, East Hill and Dead Dog Mound), whereas analyses 3 and 5 (Inspired Mound and Chowder Hill) contain less Al and trend toward a talc composition. The average calculated formula, based on analyses 1 to 5 in Table 4, is: $(Na_{0.09}Ca_{0.04}K_{0.02})$ $(Mg_{5.48}Fe^{2+}_{0.50}Al_{0.07}Mn_{0.02})$ $(Si_{7.59}Al_{0.41})O_{20}(OH)_4{\cdot}nH_2O$.

The ATEM results confirm the presence of a saponite in all samples except those from Bent Hill. There, smectite was identified as a mixed-layer mineral only. In addition to saponite, minor amounts of an Fe-rich saponite (Mg–Fe-rich smectite) were detected in Inspired and Dead Dog Mound samples, and trace amounts of an Fe-rich smectite (Fe-rich, Mg-poor smectite, variety unknown) occurs in a Chowder Hill sample. Smectite grains from Heineken Hollow were found to be chemically more heterogeneous than those from the other AAV sites. Two types were observed: the Mg-rich variety saponite, and Mg-poor smectite grains with a Si-rich core. In a few of the Mg-

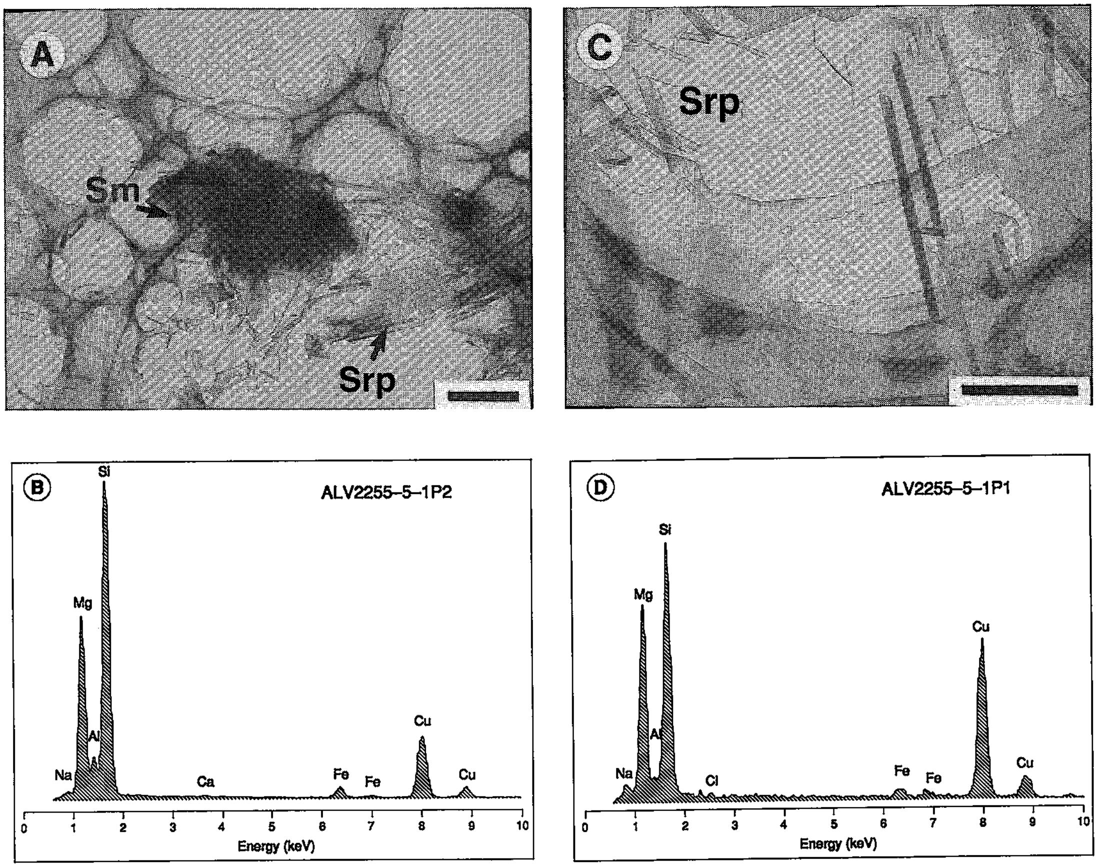

FIG. 8. A. ATEM of smectite (Sm) and serpentine (Srp) grains in sample ALV2255-1P2 (scale bar: 1.0 μm). B. EDX spectrum of Mg-rich smectite, saponite, in A. C. ATEM micrograph of serpentine from same sample. Note the curling of the grain edges due to the heat of the beam (scale bar: 0.5 μm). D. EDX spectrum of serpentine in C.

poor, Si-rich grains, a surface coating of Co was detected.

Efforts were made to identify serpentine minerals in the Central Site samples by SEM and electron microprobe, although no distinct phase was identified. Results of the SEM analyses of a grain mount are shown in Figure 7. Figure 7A shows the typical crenulated morphology of smectite, as observed in sample ALV2255-5-1P1. The EDX spectrum obtained is similar to that in Figure 7C, but contains a trace of Ca. In Figure 7B, there appear to be two different types of minerals based on morphology: a wispy, crenulated mineral and a platy mineral. The EDX spectra in Figures 7C and D suggest that these minerals have different compositions, based on their Mg:Si ratios. The wispy grains of smectite (Fig. 7C) have a lower Mg:Si ratio than the platy grains (Fig. 7D). The smectite also contains higher Al and minor Fe. The platy grains are therefore interpreted to represent the serpentine identified by XRD analysis.

The ATEM results were instructive concerning the nature of the serpentine minerals. Figure 8A shows the typical morphology of a Mg-rich smectite (EDX spectrum in Fig. 8B) that is larger (μm scale) than the adjacent serpentine grains (nm scale). Figures 8C and D show a close-up view of the grains of platy serpentine and a typical EDX spectrum, respectively. The morphology of the grains and the trace to minor amounts of Al detected in some grains, combined with the XRD traces, suggest that the serpentine is lizardite rather than chrysotile (Wicks & O'Hanley 1988). Some of the smectite grains analyzed by EDX have a composition similar to that of the serpentine grains.

DISCUSSION

A variety of silicate minerals, including phyllosilicates, has been reported from hydrothermal deposits at mid-oceanic spreading centers, but the silicates have received less attention than have the sulfides. The types of silicates and sulfides that form in active vents at bare ridge-crests depend on the composition of the hydrothermal fluids and the degree of interaction with basaltic crust and cold seawater. In sediment-covered areas, the chemically heterogeneous sediments also are involved in reactions (Koski *et al.* 1988). Silicates predicted to occur in these hydrothermal systems, based on mixing models of hydrothermal fluids with seawater, include quartz and talc (Janecky & Seyfried 1984, Bowers *et al.* 1985). Although talc is commonly reported in active hydrothermal areas (Atlantis II Deep, Red Sea: Zierenberg & Shanks 1983, Guaymas Basin: Koski *et al.* 1985, Drits *et al.* 1989, Escanaba Trough: Koski *et al.* 1988, Zierenberg & Shanks in press, East Pacific Rise: Spiess *et al.* 1980, Haymon & Kastner 1981, Styrt *et al.* 1981, Goldfarb *et al.* 1983), the amounts present are much less than those predicted for equilibrium conditions. Important controls on talc formation include temperature, water–rock ratio and degree of mixing of hot hydrothermal fluids and cold, Mg-rich seawater or pore fluids (Janecky & Seyfried 1984, Evans & Guggenheim 1988). At low activity of Si, however, either Mg-rich smectite (Zierenberg & Shanks, in press) or serpentine (Brett *et al.* 1987) may be formed over a similar range of temperature.

Iron-rich smectite (*i.e.*, nontronite) is reported to occur in sulfide deposits at numerous spreading centers (*e.g.*, Mounds Hydrothermal Field, Galapagos: Schrader *et al.* 1980, McMurtry *et al.* 1983; Atlantis II Deep, Red Sea: Cole 1983, 1988; 21°N, East Pacific Rise: Alt *et al.* 1987, Alt 1988a, b, Alt & Jiang 1991, Hekinian *et al.* 1980; TAG Hydrothermal Field, Mid-Atlantic Ridge: Thompson *et al.* 1985; Explorer Ridge: Grill *et al.* 1981). Mg-rich smectite-group minerals, such as saponite and stevensite, occur in sedimented areas such as the Guaymas Basin (Peter & Scott 1988, Drits *et al.* 1989), the Atlantis II Deep, Red Sea (Zierenberg & Shanks 1983, 1988) and Escanaba Trough (Zierenberg & Shanks, in press). Peter & Scott (1988) presented a model for the growth of chimneys in the Guaymas Basin and suggested that the first minerals to precipitate are anhydrite and stevensite, followed by pyrrhotite. Stevensite occurs in both the mounds and the chimneys, indicating formation over a large range in temperature. Zierenberg & Shanks (1983) suggested that higher temperatures and a decrease in $f(O_2)$ favor the formation of Mg-rich smectite over Fe-rich smectite and that the presence of saponite indicates Mg addition, with lower activity of Si relative to that needed for talc formation. Therefore, the dominance of saponite within the chimneys at Middle Valley is probably the result of precipitation from fluids with low $f(O_2)$ and Si activity, coupled with the influence of Mg-rich seawater.

Saponite occurs as the exclusive smectite in the northern part of the AAV and coexists with an Fe-rich saponite in the southern part. All of the clay minerals within the lining of the active chimneys were precipitated early from the fluid, in a manner similar to that in chimneys at Guaymas Basin (Peter & Scott 1988). The grain size and morphology of the chlorite support a hydrothermal origin (K. Marumo, pers. comm., 1992). Although chlorite is the dominant clay mineral in the highest-temperature vent at Chowder Hill, trace amounts of Fe-rich smectite also are present. The occurrence of chlorite, as opposed to Mg-rich smectite, requires the presence of significant amounts of Al (Evans & Guggenheim 1988) and suggests a significant contribution by sediment to the venting hydrothermal fluids at Middle Valley. The association of pyrrhotite, Fe-rich sphalerite (35–46 mole % FeS), isocubanite, chalcopyrite and arsenopyrite with saponite is consistent with formation from hydrothermal fluids with very low $f(O_2)$ and $f(S_2)$ at measured moderate temperatures and high pH (5.1–5.8) (Ames *et al.* 1993).

Minor to trace amounts of hydrothermal serpentine, both lizardite and chrysotile, have been observed in both sediment-filled rift and sediment-free mid-oceanic areas. Serpentine forms under widely varying temperatures and conditions in seafloor deposits (Styrt *et al.* 1981, Oudin 1983, Brett *et al.* 1987, Singer & Stoffers 1987, Paradis *et al.* 1988, Zierenberg & Shanks 1988). Serpentine also has been observed in sediment from the hydrothermal mound at Bent Hill (Turner *et al.* 1993). Lizardite, saponite and a mixed-layer mineral of the two components were observed in the gel-like material taken from the hydrothermal mound at Central Site, but not in the active chimneys. The mixed-layer mineral may actually be a physical mixture of discrete lizardite and saponite phases, based on the ATEM evidence (see Fig. 8A); more detailed work is needed to refine the character of this species. The gel-like nature of the material from Central Site suggests direct precipitation from fluids.

The zonation in the distribution of clay minerals in the Middle Valley hydrothermal area can be assessed from data on shallow push-core samples (Turner *et al.* 1993) and regional information on piston cores (Goodfellow *et al.* 1992), in combination with the data from chimneys in the present study. The general pattern is of dominant saponite, with traces of Fe-rich saponite and Fe-rich smectite, in actively venting chimneys, saponite and lizardite ± talc in active hydrothermal mounds, abundant smectite in talus from the flanks of the hydrothermal mounds, illite–smectite mixed-layer mineral in proximal altered sediments, smectite and a trace of an illite–smectite mixed-layer mineral in distal altered sediments, and minor smectite in unaltered sediments. In another study, Adshead (1987) identified a talc–saponite mixed-layer mineral in altered near-surface (~180 m) sediments in piston core sample 85–34, in the southern AAV (Goodfellow & Blaise 1988). In the present study, only trace amounts of talc were identified in proximal hydrothermal deposits.

The abundance of smectite decreases with increasing distance from the point of discharge of the hydrothermal fluid, consistent with a hydrothermal origin for these minerals. Turner *et al.* (1993) have determined that the Si content of the clays increases and Al content decreases with increasing distance from the hydrothermal mounds and chimneys (*e.g.*, Table 4). These trends are attributed to the lack of availability of Si in the chimneys and mounds, and to the abundance of Si in the sediment derived from diatoms, forams and detrital quartz. The Mg-rich nature of the clays in and near the areas of discharge of the hydrothermal fluid reflects the ingress of seawater into the mounds and reaction with the moderate-temperature hydrothermal fluid.

SUMMARY AND CONCLUSIONS

Clay minerals, owing to their complexity and fine-grained nature, have to date received scant attention in the study of seafloor hydrothermal massive sulfide deposits. At Middle Valley, a sediment-filled rift, the interaction of hydrothermal fluids with seawater is complicated by reactions with sediments. The types of clay minerals precipitated in the active chimneys and mounds, in association with sulfides and sulfates, provide some constraints on the formation of these deposits.

The clay minerals observed in the chimney samples from the Area of Active Venting and Bent Hill are dominated by saponite, a Mg-rich smectite. Saponite is the only smectite-group mineral in the northern part of the Area of Active Venting, but occurs with a more Fe-rich variety (Fe-rich saponite) in the southern part at Inspired and Dead Dog Mounds. The smectite from the highest-temperature vent at Chowder Hill is Fe-rich and occurs in association with chlorite. The active chimney at Bent Hill contains smectite only as a component of mixed-layer minerals. Chlorite is the dominant clay mineral in the Chowder Hill chimney, but also occurs at two other sites. The presence of chlorite implies availability of Al in the hydrothermal fluids, suggesting a contribution from proximal sediments. In the hydrothermal mound at Central Site, serpentine was detected in association with saponite in a gel-like sample. Although XRD analysis suggests the presence of a serpentine–saponite mixed-layer mineral, ATEM evidence points to a probable physical mixture of the two minerals. The Mg-rich nature of the clays in and near the areas of hydrothermal fluid discharge reflects the reaction of cold Mg-rich seawater with moderately hot hydrothermal fluids having a low $f(O_2)$ and Si activity.

ACKNOWLEDGEMENTS

The authors thank the following staff at the Geological Survey of Canada: L.K. Radburn for providing SEM photomicrographs and EDX X-ray spectra; R.N. Delabio and S. Phaneuf (Univ. Ottawa) for assistance with XRD analyses; G.J. Pringle and J.A.R. Stirling for some electron-microprobe analyses; K. Nguyen and R.D. Lancaster for computer-aided drafting. We are grateful to K. Marumo (Geological Survey of Japan) at the University of Toronto for ATEM analyses. Discussions with J.M. Franklin, M.D. Hannington, I.R. Jonasson, G.M. LeCheminant, H. Kodama (Agriculture Canada) and K. Marumo were most beneficial. Thanks to M.D. Hannington, J.A. Percival and R.A. Zierenberg (U.S. Geological Survey) for review of an earlier draft of this paper. Comments by J.C. Alt, J. Chisholm and R.F. Martin improved the manuscript and are gratefully acknowledged.

REFERENCES

ADSHEAD, J.D. (1987): Magnesium distribution and the nature of magnesium silicates in hydrothermally-altered Juan de Fuca sediments. *Trans. Am. Geophys. Union* **68**, 113 (abstr.).

ALT, J.C. (1988a): Hydrothermal oxide and nontronite deposits on seamounts in the eastern Pacific. *Marine Geol.* **81**, 227-239.

——— (1988b): The chemistry and sulfur isotope composition of massive sulfide and associated deposits on Green Seamount, eastern Pacific. *Econ. Geol.* **83**, 1026-1033.

——— & JIANG, WEI-TEH (1991): Hydrothermally precipitated mixed-layer illite–smectite in recent massive sulfide deposits from the sea floor. *Geology* **19**, 570-573.

———, LONSDALE, P., HAYMON, R. & MUEHLENBACHS, K. (1987): Hydrothermal sulfide and oxide deposits on seamounts near 21°N, East Pacific Rise. *Geol. Soc. Am. Bull.* **98**, 157-168.

AMES, D.E. & FRANKLIN, J.M. (1992): Mineralogy and geochemistry of Middle Valley hydrothermal chimneys, northern Juan de Fuca Ridge: results from Alvin dive cruise. *Geol. Surv. Can., Minerals Colloquium, Program Abstr.*, 10.

———, ——— & HANNINGTON, M.D (1993): Mineralogy and geochemistry of active and inactive chimneys and massive sulfide, Middle Valley, northern Juan de Fuca Ridge: an evolving hydrothermal system. *Can. Mineral.* **31**, 997-1024.

BOWERS, T.S., VON DAMM, K.L. & EDMOND, J.M. (1985): Chemical evolution of mid-ocean ridge hot springs. *Geochim. Cosmochim. Acta* **49**, 2239-2252.

BRETT, R., EVANS, H.T., JR., GIBSON, E.K., JR., HEDENQUIST, J.W., WANDLESS, M.-V. & SOMMER, M.A. (1987): Mineralogical studies of sulfide samples and volatile concentrations of basalt glasses from the southern Juan de Fuca Ridge. *J. Geophys. Res.* **92**, 11,373-11,379.

COLE, T.G. (1983): Oxygen isotope geothermometry and origin of smectites in the Atlantis II Deep, Red Sea. *Earth Planet. Sci. Lett.* **66**, 166-176.

——— (1988): The nature and origin of smectite in the Atlantis II Deep, Red Sea. *Can. Mineral.* **26**, 755-763.

DAVIS, E.E., GOODFELLOW, W.D., BORNHOLD, B.D., ADSHEAD, J., BLAISE, B., VILLINGER, H. & LECHEMINANT, G.M. (1987): Massive sulfides in a sedimented rift valley, northern Juan de Fuca Ridge. *Earth Planet. Sci. Lett.* **82**, 49-61.

DEER, W.A., HOWIE, R.A. & ZUSSMAN, J. (1966): *An Introduction to the Rock-Forming Minerals.* Longman Group Limited, London.

DRITS, V.A., KHVOROVA, I.V., SOKOLOVA, A.L. & VORONII, B.I. (1989): Clay minerals in deep water hydrothermal structures of the Guaymas depression (Gulf of California). *Lithology and Mineral Resources* **24**, 10-16.

EVANS, B.W. & GUGGENHEIM, S. (1988): Talc, pyrophyllite and related minerals. *In* Hydrous Phyllosilicates (Exclusive of Micas) (S.W. Bailey, ed.). *Rev. Mineral.* **19**, 225-294.

FRANKLIN, J.M., GOODFELLOW, W.D., AMES, D.E., LYDON, J.W., JONASSON, I.R. & DAVIS, E.E. (1991): Middle Valley, a major centre of hydrothermal activity in a sedimented ridge crest, northern Juan de Fuca Ridge. *Geol. Surv. Can., Current Activities Forum, Program Abstr.*, 20.

GOLDFARB, M.S., CONVERSE, D.R., HOLLAND, H.D. & EDMOND, J.M. (1983): The genesis of hot spring deposits on the East Pacific Rise, 21°N. *In* The Kuroko and Related Volcanogenic Massive Sulfide Deposits (H. Ohmoto & B.J. Skinner, eds.). *Econ. Geol., Monogr.* **5**, 184-197.

GOODFELLOW, W.D. & BLAISE, B. (1988): Sulfide formation and hydrothermal alteration of hemipelagic sediment in Middle Valley, northern Juan de Fuca Ridge. *Can. Mineral.* **26**, 675-696.

——— & THE LEG 139 SCIENTIFIC PARTY (1992): Fluid–sediment interactions associated with high temperature fluid flow, Middle Valley. *Geol. Surv. Can., Minerals Colloquium, Program Abstr.*, 7.

GRILL, E.V., CHASE, R.L., MACDONALD, R.D. & MURRAY, J.W. (1981): A hydrothermal deposit from Explorer Ridge in the northeast Pacific Ocean. *Earth Planet. Sci. Lett.* **52**, 142-150.

HAYMON, R.M. & KASTNER, M. (1981): Hot spring deposits on the East Pacific Rise at 21°N: preliminary description of mineralogy and genesis. *Earth Planet Sci. Lett.* **53**, 363-381.

HEKINIAN, R., FEVRIER, M., BISCHOFF, J.L., PICOT, P. & SHANKS, W.C. (1980): Sulfide deposits from the East Pacific Rise near 21°N. *Science* **207**, 1433-1444.

JANECKY, D.R. & SEYFRIED, W.E., JR. (1984): Formation of massive sulfide deposits on oceanic ridge crests: incremental reaction models for mixing between hydrothermal solutions and seawater. *Geochim. Cosmochim. Acta* **48**, 2723-2738.

KOSKI, R.A., LONSDALE, P.F., SHANKS, W.C., III, BERNDT, M.E. & HOWE, S.S. (1985): Mineralogy and geochemistry of a sediment-hosted hydrothermal sulfide deposit from the Southern Trough of Guaymas Basin, Gulf of California. *J. Geophys. Res.* **90**, 6695-6707.

———, SHANKS, W.C., III, BOHRSON, W.A. & OSCARSON, R.L. (1988): The composition of massive sulfide deposits from the sediment-covered floor of Escanaba Trough, Gorda Ridge: implications for depositional processes. *Can. Mineral.* **26**, 655-673.

MCMURTRY, G.M., WANG, CHUNG-HO & YEH, HSUEH-WEN (1983): Chemical and isotopic investigations into the origin of clay minerals from the Galapagos hydrothermal mounds field. *Geochim. Cosmochim. Acta* **47**, 475-489.

MOORE, D.M. & REYNOLDS, R.C., JR. (1989): *X-Ray Diffraction and the Identification and Analysis of Clay Minerals.* Oxford University Press, Inc., New York.

OUDIN, E. (1983): Hydrothermal sulfide deposits of the East Pacific Rise (21° N). I. Descriptive mineralogy. *Marine Mining* **4**, 39-72.

PARADIS, S., JONASSON, I.R., LECHEMINANT, G.M. & WATKINSON, D.H. (1988): Two zinc-rich chimneys from the Plume Site, southern Juan de Fuca Ridge. *Can. Mineral.* **26**, 637-654.

PETER, J.M. & SCOTT, S.D. (1988): Mineralogy, composition, and fluid-inclusion microthermometry of seafloor hydrothermal deposits in the southern trough of Guaymas Basin, Gulf of California. *Can. Mineral.* **26**, 567-587.

SCHRADER, E.L., ROSENDAHL, B.R., FURBISH, W.J. & MATTEY, D.P. (1980): Mineralogy and geochemistry of hydrothermal and pelagic sediments from the Mounds Hydrothermal Field, Galapagos spreading center: DSDP leg 54. *J. Sed. Petrol.* **50**, 917-928.

SINGER, A. & STOFFERS, P. (1987): Mineralogy of a hydrothermal sequence in a core from the Atlantis II Deep, Red Sea. *Clay Mineral.* **22**, 251-267.

SPIESS, F.N., MACDONALD, K.C., ATWATER, T., BALLARD, R., CARRANZA, A., CORDOBA, D., COX, C., DIAZ-GARCIA, V.M., FRANCHETEAU, J., GUERRERO, J., HAWKINS, J., HAYMON, R., HESSLER, R., JUTEAU, T., KASTNER, M., LARSON, R., LUYENDYK, B., MACDOUGALL, J.D., MILLER, S., NORMARK, W., ORCUTT, J. & RANGIN, C. (1980): East

Pacific Rise: hot springs and geophysical experiments. *Science* **207**, 1421-1433.

STYRT, M.M., BRACKMANN, A.J., HOLLAND, H.D., CLARK, B.C., PISUTHA-ARNOND, V., ELDRIDGE, C.S. & OHMOTO, H. (1981): The mineralogy and the isotopic composition of sulfur in hydrothermal sulfide/sulfate deposits on the East Pacific Rise, 21°N latitude. *Earth Planet. Sci. Lett.* **53**, 382-390.

THOMPSON, G., MOTTL, M.J. & RONA, P.A. (1985): Morphology, mineralogy and chemistry of hydrothermal deposits from the TAG area, 26°N Mid-Atlantic Ridge. *In* Water-Rock Interaction (Y. Kitano, ed.). *Chem. Geol.* **49**, 243-257.

TURNER, R.J.W., AMES, D.E., GOODFELLOW, W.D., LEITCH, C.H.B., FRANKLIN, J.M. & HOY, T. (1993): Character of active hydrothermal mounds and nearby altered hemipelagic sediments in the hydrothermal areas of Middle Valley, northern Juan de Fuca Ridge: shallow core data. *Can. Mineral.* **31**, 973-995.

WICKS, F.J. & O'HANLEY, D.S. (1988): Serpentine minerals: structures and petrology. *In* Hydrous Phyllosilicates (Exclusive of Micas) (S.W. Bailey, ed.). *Rev. Mineral.* **19**, 91-167.

ZIERENBERG, R.A. & SHANKS, W.C., III (1983): Mineralogy and geochemistry of epigenetic features in metalliferous sediment, Atlantis II Deep, Red Sea. *Econ. Geol.* **78**, 57-72.

________ & ________ (1988): Isotopic studies of epigenetic features in metalliferous sediment, Atlantis II Deep, Red Sea. *Can. Mineral.* **26**, 737-753.

________ & ________ (in press): Sediment alteration associated with massive sulfide formation in the Escanaba Trough, Gorda Ridge: the importance of seawater mixing and magnesium metasomatism. *U.S. Geol. Surv., Bull.* **2022**.

Received May 22, 1992, revised manuscript accepted July 11, 1993.